Article

Thermally Cross-Linked Superparamagnetic Iron Oxide Nanoparticles: Synthesis and Application as a Dual Imaging Probe for Cancer in Vivo

Haerim Lee, Mi Kyung Yu, Sangjin Park, Sungmin Moon, Jung Jun Min, Yong Yeon Jeong, Hae-Won Kang, and Sangyong Jon

J. Am. Chem. Soc., **2007**, 129 (42), 12739-12745• DOI: 10.1021/ja072210i • Publication Date (Web): 25 September 2007

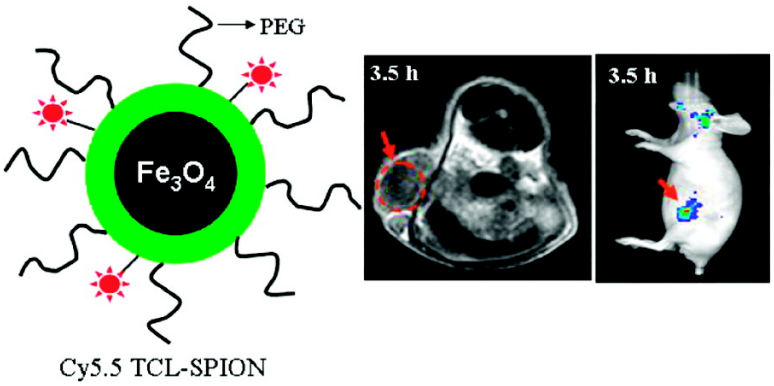

More About This Article

Additional resources and features associated with this article are available within the HTML version:

- Supporting Information
- Links to the 12 articles that cite this article, as of the time of this article download
- Access to high resolution figures
- Links to articles and content related to this article
- Copyright permission to reproduce figures and/or text from this article

View the Full Text HTML

J|A|C|S
ARTICLES
Published on Web 09/25/2007

Thermally Cross-Linked Superparamagnetic Iron Oxide Nanoparticles: Synthesis and Application as a Dual Imaging Probe for Cancer in Vivo

Haerim Lee,[†] Mi Kyung Yu,[†] Sangjin Park,[†] Sungmin Moon,[‡] Jung Jun Min,[‡] Yong Yeon Jeong,*[,‡] Hae-Won Kang,[§] and Sangyong Jon*[,†]

Contribution from the Research Center for Biomolecular Nanotechnology, Department of Life Science, GIST, 1 Oryong-dong, Buk-gu, Gwangju 500-712 Republic of Korea, Department of Diagnostic Radiology, Chonnam National University Medical School, Gwangju 501-746 Korea, and Department of Radiology, University of Massachusetts Medical School, Worcester, Massachusetts 01604

Received March 29, 2007; E-mail: syjon@gist.ac.kr; yjeong@jnu.ac.kr

Abstract: We report the fabrication and characterization of thermally cross-linked superparamagnetic iron oxide nanoparticles (TCL-SPION) and their application to the dual imaging of cancer in vivo. Unlike dextran-coated cross-linked iron oxide nanoparticles, which are prepared by a chemical cross-linking method, TCL-SPION are prepared by a simple, thermal cross-linking method using a Si−OH-containing copolymer. The copolymer, poly(3-(trimethoxysilyl)propyl methacrylate-*r*-PEG methyl ether methacrylate-*r*-*N*-acryloxysuccinimide), was synthesized by radical polymerization and used as a coating material for as-synthesized magnetite (Fe_3O_4) SPION. The polymer-coated SPION was further heated at 80 °C to induce cross-linking between the $-Si(OH)_3$ groups in the polymer chains, which finally generated TCL-SPION bearing a carboxyl group as a surface functional group. The particle size, surface charge, presence of polymer-coating layers, and the extent of thermal cross-linking were characterized and confirmed by various measurements, including dynamic light scattering, Fourier transform infrared spectroscopy, and X-ray photoelectron spectroscopy. The carboxyl TCL-SPION was converted to amine-modified TCL-SPION and then finally to Cy5.5 dye-conjugated TCL-SPION for use in dual (magnetic resonance/optical) in vivo cancer imaging. When the Cy5.5 TCL-SPION was administered to Lewis lung carcinoma tumor allograft mice by intravenous injection, the tumor was unambiguously detected in T_2-weighted magnetic resonance images as a 68% signal drop as well as in optical fluorescence images within 4 h, indicating a high level of accumulation of the nanomagnets within the tumor site. In addition, ex vivo fluorescence images of the harvested tumor and other major organs further confirmed the highest accumulation of the Cy5.5 TCL-SPION within the tumor. It is noteworthy that, despite the fact that TCL-SPION does not bear any targeting ligands on its surface, it was highly effective for tumor detection in vivo by dual imaging.

Introduction

Superparamagnetic iron oxide nanoparticles (SPION) are an emerging form of nanomedicine[1] for the treatment of various diseases including cancer because they can be used as magnetic resonance (MR) contrast agents[2−10] and can be incorporated into magnetic field-guided drug delivery vehicles for cancer treatment.[12−14] Several requirements must be met for SPION to be successfully used in MR imaging in vivo: (i) good dispersibility in physiological medium, (ii) biocompatibility, and (iii) an anti-biofouling property that prevents adsorption of plasma proteins or cells onto their surface. Therefore, it is necessary to engineer the surface of SPION to minimize such biofouling and aggregation under harsh physiological conditions

[†] Gwangju Institute of Science and Technology.
[‡] Chonnam National University Medical School.
[§] University of Massachusetts Medical School.

(1) (a) Farokhzad, O. C.; Langer, R. *Adv. Drug Deliv. Rev.* **2006**, *58*, 1456−1459. (b) Wagner, V.; Dullaart, A.; Bock, A.−K.; Zweck, A. *Nat. Biotech.* **2006**, *24*, 1211−1217. (c) Ferrari, M. *Nat. Rev. Cancer* **2005**, *5*, 161−171.
(2) Corot, C.; Robert, P.; Idee, J. M.; Port, M. *Adv. Drug Deliv. Rev.* **2006**, *58*, 1471−1504.
(3) Thorek, D. L.; Chen, A. K.; Czupryna, J.; Tsourkas, A. *Ann. Biomed. Eng.* **2006**, *34*, 23−38.
(4) Weissleder, R. *Science* **2006**, *312*, 1168−1171.
(5) (a) Lee, J. H.; et al. *Nat. Med.* **2006**, *13*, 95−99. (b) Huh, Y. M.; Jun, Y. W.; Song, H. T.; Kim, S.; Choi, J. S.; Lee, J. H.; Yoon, S.; Kim, K. S.; Shin, J. S.; Suh, J. S.; Cheon, J. *J. Am. Chem. Soc.* **2005**, *127*, 12387−12391.
(6) Funovics, M. A.; Kapeller, B.; Hoeller, C.; Su, H. S.; Kunstfeld, R.; Puig, S.; Macfelda, K. *Magn. Reson. Imaging* **2004**, *22*, 843−850.
(7) Martina, M. S.; Fortin, J. P.; Menager, C.; Clement, O.; Barratt, G.; Grabielle-Madelmont, C.; Gazeau, F.; Cabuil, V.; Lesieur, S. *J. Am. Chem. Soc.* **2005**, *127*, 10676−10685.
(8) Weinmann, H. J.; Ebert, W.; Misselwitz, B.; Schmitt-Willich, H. *Eur. J. Radiol.* **2003**, *46*, 33−44.
(9) Harisinghani, M. G.; Barentsz, J.; Hahn, P. F.; Deserno, W. M.; Tabatabaei, S.; van de Kaa, C. H.; de la Rosette, J.; Weissleder, R. *N. Engl. J. Med.* **2003**, *348*, 2491−2499.
(10) de Vries, I. J.; et al. *Nat. Biotechnol.* **2005**, *23*, 1407−1413.
(11) Ito, A.; Kuga, Y.; Honda, H.; Kikkawa, H.; Horiuchi, A.; Watanabe, Y.; Kobayashi, T. *Cancer Lett.* **2004**, *212*, 167−175.
(12) Kohler, H.; Sun, C.; Wang, J.; Zhang, M. *Langmuir* **2005**, *21*, 8858−8864.
(13) Nasongkla, N.; et al. *Nano Lett.* **2006**, *6*, 2427−2430.
(14) Kim, J.; et al. *Angew. Chem., Int. Ed.* **2006**, *45*, 7754−7758.

(i.e., high salt and protein concentrations).[15−22] Several synthetic and natural polymers have been employed to coat the surface of SPION.[15,16,21,22] These polymers include dextran,[23,24] polyethylene glycols (PEGs),[12,15,16,25] and polyvinylpyrrolidone,[16,26] all of which are known to be biocompatible and all of which promote good dispersion of SPION in aqueous medium; however, the possibility that the polymer coating can be lost under harsh in vivo conditions has been a concern.[16,21,22]

To ensure the stability of the polymer coating in vivo, cross-linked iron oxide nanoparticles (CLIO) had been developed.[23,27] CLIO are composed of dextran-coated SPION in which the dextran polymer chains are chemically cross-linked. These nanoparticles have been widely used for in vivo as well as in vitro MR imaging.[28−31] Although CLIO are considered one of the most promising MR contrast agents because of their stable coating, anti-biofouling property, biocompatibility, and small hydrodynamic size, multiple synthetic and purification steps are needed to obtain the final, functionalized SPION, namely (i) dextran coating and purification, (ii) cross-linking using epichlorohydrin and purification, and (iii) chemical treatment to introduce functional groups such as amines and aldehydes onto the nanoparticle surface.[29] Furthermore, there is a concern that the unreacted residual chemical reagents in CLIO will be toxic in vivo.

Very recently, we reported anti-biofouling polymer-coated SPION and described their use as a MR contrast agent for in vivo cancer imaging.[15] The polymer employed in the study, poly(3-(trimethoxysilyl)propyl methacrylate-*r*-PEG methyl ether methacrylate) [denoted as poly(TMSMA-*r*-PEGMA)] was composed of "a surface-reactive function ($-Si(OMe)_3$)" and "a protein-repelling function (PEG)".[32,33] We demonstrated that the polymer coating on SPION (Fe_3O_4) is highly stable in physiological medium and resistant to protein adsorption in vitro and that the coated SPION allowed efficient detection of cancer in vivo when used for clinical MR imaging.[15] Unlike CLIO, a stable, firm polymer coating layer on SPION was generated by thermal cross-linking and without the need for chemicals or additional synthetic steps. It was possible to obtain this highly stable polymer coating because the PEG−silane copolymer becomes cross-linked by simple heat treatment through condensation of hydrolyzed silane groups ($-Si(OH)_3$).[33] Unlike CLIO, however, this system did not allow the inclusion of a functional group through which additional features such as active targeting and multimodal imaging can be introduced.[34,35] In the current study, therefore, we produced and characterized functionalized, thermally cross-linked SPION (TCL-SPION). Furthermore, to demonstrate its applicability as a novel imaging nanoprobe we report the successful use of near-infrared dye-conjugated TCL-SPION for dual (optical/MR) imaging of cancer in vivo.

Experimental Section

Materials. *N*-Acryloxysuccinimide (NAS; 99%) was purchased from ACROS Organics (Noisy-le-Grand, France). Cy5.5 mono NHS ester was obtained from Amersham Biosciences (Succursale, France). 3-(Trimethoxysilyl)propyl methacrylate (TMSMA; 98%), poly(ethylene glycol) methyl ether methacrylate (PEGMA; average $M_n = \sim 475$), tetrahydrofuran (anhydrous, 99.9%, inhibitor-free), 2,2′-azobisisobutyronitrile (98%), ferric chloride hexahydrate ($FeCl_3 \cdot 6H_2O$), ferrous chloride tetrahydrate ($FeCl_2 \cdot 4H_2O$), 2,2′-(ethylenedioxy)bis-(ethylamine) (98%), 1-ethyl-3-(3-dimethylaminopropyl)carbodiimide hydrochloride (commercial grade), *N*-hydroxysuccinimide (98%), Sephadex G-50, dimethyl sulfoxide, and paraformaldehyde were purchased from Sigma-Aldrich Chemical Co. (St. Louis, MO). Ammonium hydroxide solution (~28% in water) was purchased from Fluka (Buchs, Switzerland). Other organic solvents were used as received. A rare-earth magnet (N35 grade, cylinder type, 5 cm diameter × 2 cm height) was purchased from Daehan-Magnet Co. (Seoul, South Korea).

Measurements. The saturation magnetization (M_s) value of TCL-SPION was measured at 300 K using a magnetic property measurement system (Quantum Design, San Diego, CA). The applied magnetic field was varied from 10,000 to −10,000 Oe. The saturation magnetization in emu/g was normalized by the wt % of magnetite derived from thermogravimetric analysis (TGA) to obtain the emu/g of iron. To confirm cross-linking between entangled polymer chains on carboxyl TCL-SPION, X-ray photoelectron spectroscopy (XPS) was performed using a MultiLab 2000 (VG, East Grinstead, UK) with a non-monochromatic Mg Kα radiation X-ray source (300 W), an incident angle of 65°, and an emission incident angle of 0°. An analyzer pass energy of 20 eV was used to enable higher resolution (narrow) scans. The hydrodynamic particle sizes and zeta-potentials of carboxyl, amino, and Cy5.5 TCL-SPION were measured using an ELS 8000 electrophoretic light-scattering apparatus (Otsuka Electronics Korea, Seoul, South Korea). The size and dispersion quality of carboxyl and amino TCL-SPION were investigated by transmission electron microscopy

(15) Lee, H.; Lee, E.; Kim D. K.; Jang, N. K.; Jeong, Y. Y.; Jon, S. *J. Am. Chem. Soc.* **2006**, *128*, 7383−7389.
(16) Gupta, A. K.; Gupta, M. *Biomaterials* **2005**, *26*, 3395−4021.
(17) Mikhaylova, M.; Kim, D. K.; Bobraysheva, N.; Osmolowsky, M.; Semenov, V.; Tsakalakos, T.; Muhammed, M. *Langmuir* **2004**, *20*, 2472−2477.
(18) Kohler, N.; Fryxell, G. E.; Zhang, M. *J. Am. Chem. Soc.* **2004**, *126*, 7206−7211.
(19) Gupta, A. K.; Curtis, A. S. *J. Mater. Sci.: Mater. Med.* **2004**, *15*, 493−496.
(20) Raynal, I.; Prigent, P.; Peyramaure, S.; Najid, A.; Rebuzzi, C.; Corot, C. *Invest. Radiol.* **2004**, *39*, 56−63.
(21) Zhang, Y.; Kohler, N.; Zhang, M. *Biomaterials* **2002**, *23*, 1553−1561.
(22) Moghimi, S. M.; Hunter, A. C.; Murray, J. C. *Pharmacol. Rev.* **2001**, *53*, 283−318.
(23) Wang, Y.-X. J.; Hussain, S. M.; Krestin, G. P. *Eur. Radiol.* **2001**, *11*, 2319−2331.
(24) Berry, C. C.; Wells, S.; Charles, S.; Aitchison, G.; Curtis, A. S. *Biomaterials* **2004**, *25*, 5405−5413.
(25) Kim, D. K.; Mikhaylova, M.; Wang, F. H.; Kehr, J.; Bjelke, B.; Zhang, Y.; Tsakalakos, T.; Muhammed, M. *Chem. Mat.* **2003**, *15*, 4343−4351.
(26) D'Souza, A. J.; Schwen, R. L.; Topp, E. M. *J. Control. Release* **2004**, *94*, 91−100.
(27) Wunderbaldinger, P.; Josephson, L.; Weissleder, R. *Acad. Radiol.* **2002**, *Suppl 2*, S304−306.
(28) Moore, A.; Marecos, E.; Bogdanov, A. Jr.; Weissleder, R. *Radiology* **2000**, *214*, 568−574.
(29) Josephson, L.; Tung, C. H.; Moore, A.; Weissleder, R. *Bioconjugate Chem.* **1999**, *10*, 186−191.
(30) Choi, H.; Choi, S. R.; Zhou, R.; Kung, H. F.; Chen, I. *W. Acad. Radiol.* **2004**, *11*, 996−1004.
(31) Tsourkas, A.; Shinde-Patil, V. R.; Kelly, K. A.; Patel, P.; Wolley, A.; Allport, J. R.; Weissleder, R. *Bioconjugate Chem.* **2005**, *16*, 576−581.
(32) Jon, S.; Seong, J.; Khademhosseini, A.; Tran, T. T.; Laibinis, P. E.; Langer, R. *Langmuir* **2003**, *19*, 9889−9893.
(33) (a) Khademhosseini, A.; Jon, S.; Suh, K. Y.; Tran, T. −N. T.; Eng, G.; Yeh, J.; Seong, J.; Langer, R. *Adv. Mater.* **2003**, *15*, 1995−2000. (b) Khademhosseini, A.; Suh, K. Y.; Jon. S.; Eng, G.; Yeh, J.; Chen. G. J.; Langer, R. *Anal. Chem.* **2004**, *76*, 3675−3681.
(34) (a) Josephson, L.; Kircher, M. F.; Mahmood, U.; Tang, Y.; Weissleder, R. *Bioconjugated Chem.* **2002**, *13*, 554−560. (b) Weissleder, R.; Kelly, K.; Sun, E. Y.; Shtatland, T.; Josephson, L. *Nat. Biotechnol.* **2005**, *23*, 1418−1423. (c) Lewin, M.; Carlesso, N.; Tung, C. H.; Tang, X. W.; Cory, D.; Scadden, D. T.; Weissleder, R. *Nat. Biotechnol.* **2000**, *18*, 410−414.
(35) (a) Moore, A.; Medarova, Z.; Potthast, A.; Dai, G. *Cancer Res.* **2004**, *64*, 1821−1827. (b) Kim, S.; et al. *Nat. Biotechnol.* **2004**, *22*, 93−97. (c) Veiseh, O.; et al. *Nano Lett.* **2005**, *5*, 1003−1008. (d) Talanov, V. S.; Regino, C. A.; Kobayashi, H.; Bernardo, M.; Choyke, P. L.; Brechbiel, M. W. *Nano Lett.* **2006**, *6*, 1459−1463. (e) Mulder, W. J.; Koole, R.; Brandwijk, R. J.; Storm, G.; Chin, P. T.; Strijkers, G. J.; de Mello Donega, C.; Nicolay, K.; Griffioen, A. W. *Nano Lett.* **2006**, *6*, 1−6. (f) Orlova, A.; et al. *Cancer Res.* **2006**, *66*, 4339−4348. (g) Lee, J. H.; Jun, Y. W.; Yeon, S. I.; Shin, J. S.; Chen, J. *Angew. Chem., Int. Ed.* **2006**, *45*, 8160−8162. (h) Vuu, K.; Xie, J.; McDonald, M. A.; Bernardo, M.; Hunter, F.; Zhang, Y.; Li, K.; Bednarski, M.; Guccione, S. *Bioconjugate Chem.* **2005**, *16*, 995−999. (i) Kircher, M. F.; Mahmood, U.; King, R. S.; Weissleder, R.; Josephson, L. *Cancer Res.* **2003**, *63*, 8122−8125.

(TEM) using a TECNAI F20 electron microscope (Philips Electronic Instruments Corp., Mahwah, NJ) operated at 200 kV. For TEM sample preparation, carboxyl and amino TCL-SPION were diluted and deposited on a carbon-coated copper grid and allowed to air-dry.

Synthesis of Poly(TMSMA-*r*-PEGMA-*r*-NAS).[32] TMSMA (11.2 mmol, 2.78 g, 1 equiv), PEGMA (11.2 mmol, 5.32 g, 1 equiv), and NAS (9.6 mmol, 1.62 g, 0.86 equiv) were dissolved in 25 mL of THF (anhydrous, 99.9%, inhibitor-free). This mixture was degassed for 15 min by bubbling with N_2. After adding 0.32 mmol of 2,2′-azo-bis-isobutyronitrile (53 mg, 0.01 equiv) as a radical initiator, the vial was sealed with a Teflon-lined screw cap. The polymerization reaction was carried out at 70 °C for 24 h. The final product solution was stored at 4 °C. ^{1}H NMR (300.40 MHz, $CDCl_3$): $\delta = 4.13$ (br, 2H, CO_2-CH_2 of PEGMA), 3.92 (br, 2H, CO_2-CH_2 of TMSMA), 3.66 (s, 30H), 3.63−3.55 (s, 9H; m, 2H), 3.40 (s, 3H), 2.82 (br, 4H, CO-CH_2 of NAS), 2.0−1.71 (br, 6H), 1.04 (br, 2H), 0.87 (br, 4H), 0.66 (br, 2H). $M_n = 16\,274$ and $M_w = 26\,795$ with a polydispersity of 1.646 as measured by gel permeation chromatography using a Waters 1515 isocratic pump and a Waters 2414 Refractive Index detector. THF was used as the eluent and delivered at a flow rate of 0.4 mL/min.

Synthesis of Carboxyl TCL-SPION. $FeCl_3 \cdot 6H_2O$ (0.5 g, 1.85 mmol) and $FeCl_2 \cdot 4H_2O$ (0.184 g, 0.925mmol) were dissolved in deoxygenated distilled water (30 mL) that had been degassed by bubbling with N_2 for 20 min. To this solution was added 7.5 mL of NH_4OH (∼28% in water) under N_2 atmosphere while stirring vigorously for 30 min. At this time, the pH of the mixture changed from approximately 2.3 to above 10.5, and the color changed to deep black, indicating the formation of iron oxide particles. To remove the remaining salt in the solution, an external magnetic field (M_{ext}) was applied to the solution using a rare-earth magnet. Within a few minutes all of the black particles sank toward the magnet, and the resulting supernatant was discarded. Distilled water (30 mL) was added to the black precipitate, and the mixture was stirred gently to redisperse the particles. The particles were washed three times by applying M_{ext}, followed by removal of the supernatant. After discarding the supernatant, 250 mg of **1** (hydrolyzed form of poly(TMSMA-*r*-PEGMA-*r*-NSA)) in 30 mL of distilled water was added, and the mixture was stirred for 1 h. After several washing steps to remove the remaining polymer, the solution was sonicated in 30 mL of distilled water for 30 min at 200 W using a VCX-500 Ultrasonic Processor (Sonics & Materials, Inc., Newtown, CT). Next, M_{ext} was applied again overnight to precipitate the aggregated particles. Most of the particles remained in the supernatant, but a small portion precipitated. The supernatant was carefully collected and then heated at 80 °C for 2 h to achieve cross-linking between entangled polymer chains on the particle surface. The resulting thermally cross-linked poly(TMSMA-*r*-PEGMA-*r*-NAS)-coated SPION (TCL-SPION) were centrifuged at 6000 rpm (3580*g*) for 10 min, followed by 10 000 rpm (9950*g*) for 10 min to further remove very small aggregates. The resulting carboxyl TCL-SPION was stored at 4 °C until use in experiments.

Synthesis of Amino TCL-SPION. 2,2′-(Ethylenedioxy) bis-(ethylamine) (98%; 0.2 mL of 1 M) and 1-ethyl-3-(3-dimethylaminopropyl) carbodiimide hydrochloride (1 mL of 100 mM) were added successively to 1 mL of carboxyl TCL-SPION (24 mg SPION/mL) and vortexed vigorously. After 2.5 h, the solution was dialyzed against distilled water using a 100-kDa molecular mass cutoff dialysis membrane (Spectrum Laboratories Inc., Rancho Dominguez, CA) for 2 days to synthesize amine-modified TCL-SPION (amino TCL-SPION). The synthesis of amino TCL-SPION was confirmed by measuring the surface zeta-potential change between carboxyl and amino TCL-SPION using the ELS 8000 electrophoretic light-scattering apparatus. The resulting amino TCL-SPION was stored at 4 °C until use.

Synthesis of Cy5.5-Conjugated TCL-SPION. Cy5.5 mono-NHS ester (2 mg) dissolved in 400 μL of dimethyl sulfoxide was added slowly to 1 mL of amino TCL-SPION (14 mg SPION/mL) and reacted on ice in the dark with vigorous stirring. After 4 h, unreacted free Cy5.5 was removed by gel filtration on Sephadex G-50. The resulting Cy5.5 TCL-SPION was stored at 4 °C in the dark until use. Quantitative analysis of the amount of conjugated Cy5.5 per milligram of SPION was determined by measuring the fluorescence intensity using an RF-5301PC spectrofluorometer (Shimadzu, Kyoto, Japan).

Cell Culture and Preparation. Lewis lung carcinoma (LLC) cells (American Type Culture Collection, Manassas, VA) were grown as a monolayer in a humidified incubator in a 95% air/5% CO_2 atmosphere at 37 °C in Petri dish (Nunc, Naperville, IL) containing Dulbecco's Modified Eagle's Medium (GIBCO, Grand Island, NY) supplemented with 10% (v/v) heat-inactivated fetal bovine serum (GIBCO), 100 IU/mL penicillin (GIBCO), and 100 IU/mL streptomycin (GIBCO). For experiments, LLC cells were detached mechanically and adjusted to the required concentration of viable cells as determined by counting in a hemocytometer.

In Vivo MR and Optical Imaging. For all animals, MR and optical images were taken prior to and at selected time points after injection of Cy5.5 TCL-SPION. Mice were anesthetized by inhalation of 1.5% isoflurane in 1:2 O_2/N_2. The Cy5.5 TCL-SPION was injected intravenously through the tail vein. MR imaging was performed with a 1.5-T MR scanner (GE Signa Excite Twin-speed; GE Health Care, Milwaukee, WI) and using an animal coil (4.3-cm Quadrature Volume Coil; Nova Medical System, Wilmington, DE). For imaging of mice, T_2-weighted fast spin−echo was performed under the following conditions: time of repetition/time of echo, 4200/102 ms; flip angle, 90°; echo train length, 10; field of view, 5 cm; section thickness, 2 mm; intersection gap, 0.2 mm; matrix, 256 × 160.

Quantitative analysis of MR images was performed by a single radiologist. The signal intensity (SI) was measured in defined regions of interest (ROIs), which were in similar locations within the tumor center. In addition, the SI of ROIs in the back muscle adjacent to the tumor was measured. The size of each ROI was two-thirds the maximum diameter of the tumor. Relative signal enhancement was calculated by using SI measurements before (SI pre) and 3.5 h after (SI post) injection of Cy5.5 TCL-SPION according to the following formula: relative signal enhancement (%) = 100 × [1-(SI post in tumor/SI post in muscle)/(SI pre in tumor/SI pre in muscle)], where SI pre-lesion signal intensity on pre-enhanced scan (control) and SI post-lesion signal intensity on post-enhanced scan at 3.5 h.

Optical imaging was performed using an IVIS 100 imaging system (Xenogen Corp., Alameda, CA). The optical images were obtained 0 h, 1 h 45 min, and 3 h 30 min after injection of Cy5.5 TCL-SPION. Optical images were acquired using an exposure time of 1 s and via the Cy5.5 filter channel.

Results and Discussion

To introduce a functional group onto the surface of TCL-SPION, we redesigned the previous poly(TMSMA-*r*-PEGMA).[32] PEG is needed for its anti-biofouling property, and silane part is needed to cross-link the polymer coating in TCL-SPION.[33] Thus, we simply added an additional functional group, a carboxylic acid in activated form with *N*-hydroxysuccinimide, to the poly(TMSMA-*r*-PEGMA) by incorporating the corresponding monomer during radical polymerization (Figure 1). ^{1}H NMR revealed that the resulting random copolymer, poly(TMSMA-*r*-PEGMA-*r*-NAS), contains a similar molar ratio of PEG, $-Si(OCH_3)_3$, and NHS-activated carboxylic acid (1:0.85:0.71) as the initial feed ratio (1:1:0.86) prior to polymerization (see Supporting Information, Figure S1). We chose the NHS-activated form of acrylic acid as a monomer because a polymeric gel was produced instead of the desired copolymer when the unprotected acrylic acid was used, presumably due to acid (COOH)-mediated cross-linking between partially hydrolyzed silane groups during radical polymerization at high temperature.[36]

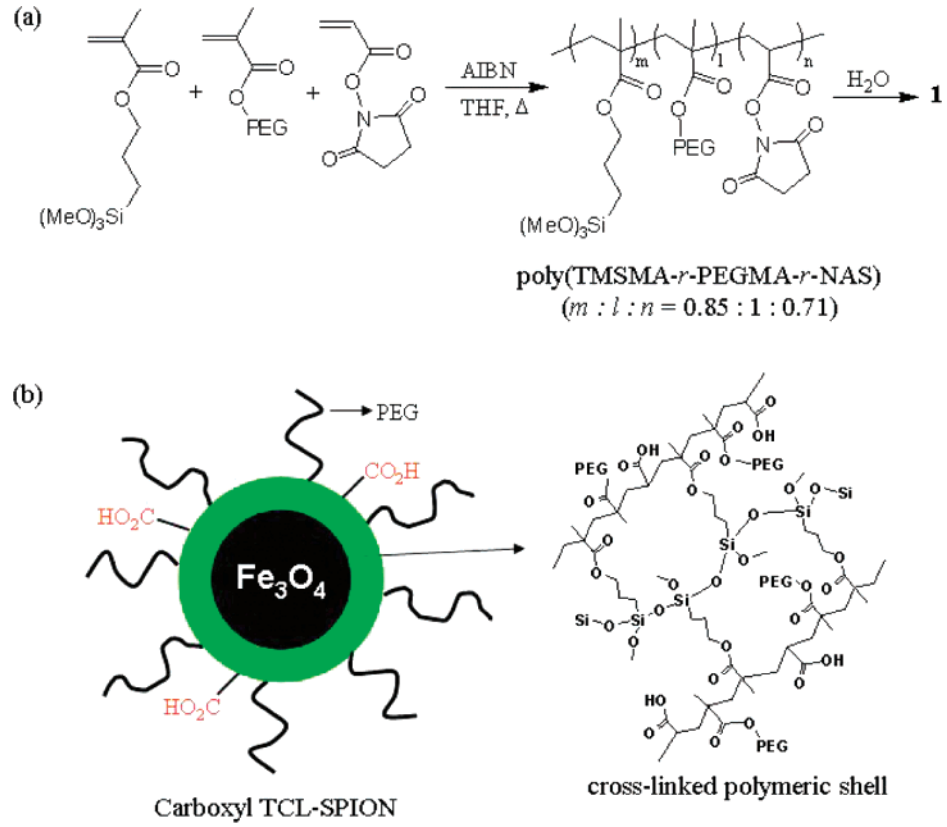

Figure 1. (a) Synthetic scheme for the production of poly(TMSMA-*r*-PEGMA-*r*-NAS). (b) Schematic illustration of carboxyl TCL-SPION showing cross-linking between polymer layers after heat treatment.

The poly(TMSMA-*r*-PEGMA-*r*-NAS) was hydrolyzed in water prior to use as a coating material of the as-synthesized magnetite (Fe_3O_4) nanoparticles. During the hydrolysis process, trimethoxysilane and NHS ester are spontaneously converted to trihydroxysilane and carboxylic acid, respectively. The resulting polymer-coated SPION was prepared by our previously described stepwise coating method, which involves (i) generation of a magnetite core (Fe_3O_4), (ii) polymer coating, and (iii) purification.[15] The polymer-coated SPION was dispersed in water and then heated at 80 °C for 2 h to cross-link the polymer coating layer, resulting in TCL-SPION with a carboxyl group as a surface functional group. This preparation of carboxyl TCL-SPION is simpler and easier to carry out than the preparation of CLIO.

We next characterized the carboxyl TCL-SPION, including analysis of the particle size, surface charge, and strength of magnetization. Dynamic light-scattering (DLS) measurements revealed that the carboxyl TCL-SPION had a relatively narrow size distribution with mean size of 25.6 ± 2.7 nm (Figure 2), which is similar to or smaller than conventional dextran-coated types of SPION such as CLIO[23,27] and monocrystalline iron oxide nanoparticle (MION).[6,37] Because DLS provides information on the hydrodynamic particle size of whole-particle clusters, including polymer coating layers and the magnetite core, we examined the size of the iron oxide core alone by TEM. As shown in Figure 2, the magnetite cores ranged from approximately 3 to 10 nm, indicating that the TLC-SPION were

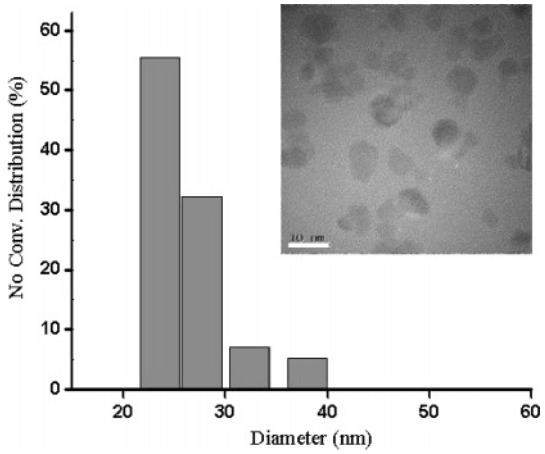

Figure 2. Hydrodynamic size distribution graph along with TEM image of carboxyl TCL-SPION. The scale bar in the TEM image corresponds to 10 nm.

coated with a layer of polymer that was less than 10 nm thick. FT-IR spectroscopy of lyophilized carboxyl TCL-SPION confirmed the presence of the polymer in the nanoparticles, with characteristic peaks of hydrolyzed poly(TMSMA-*r*-PEGMA-*r*-NAS) around 1720, 1105, and 627 cm^{-1}, which correspond to stretching bands of C═O, C−O, and Si−O, respectively (Figure S2, Supporting Information). TGA further revealed that the polymer accounted for approximately 19% (w/w) of the carboxyl TCL-SPION (Figure S3, Supporting Information). Together, these results confirm the presence of a polymer coating on the SPION. When the magnetic moment was measured as a function of applied field at 300 K, the carboxyl TCL-SPION exhibited superparamagnetic behaviors showing

(36) Linssen, T.; Cassiers, K.; Cool, P.; Vansant, E. F. *Adv. Colloid Interface Sci.* **2003**, *103*, 121−147.
(37) Weissleder, R.; Lee, A. S.; Khaw, B. A.; Shen, T.; Brady, T. J. *Radiology* **1992**, *182*, 381−385.

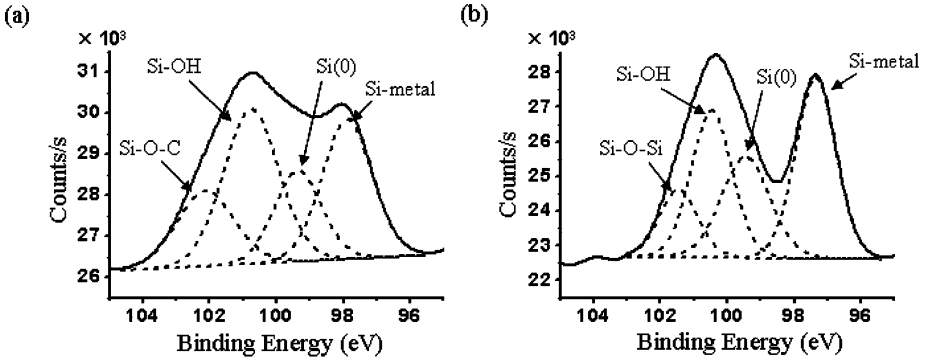

(c)

	composition (%)				
	Si-metal	Si(0)	Si-OH	Si-O-C	Si-O-Si
before heat treatment	29.0	17.8	35.3	17.9	0
after heat treatment	35.0	23.6	28.9	0	12.5

Figure 3. High-resolution Si(2p) XPS data for carboxyl TCL-SPION before (a) and after (b) heat treatment at 80 °C for 2 h, and the relative atomic composition is summarized in (c).

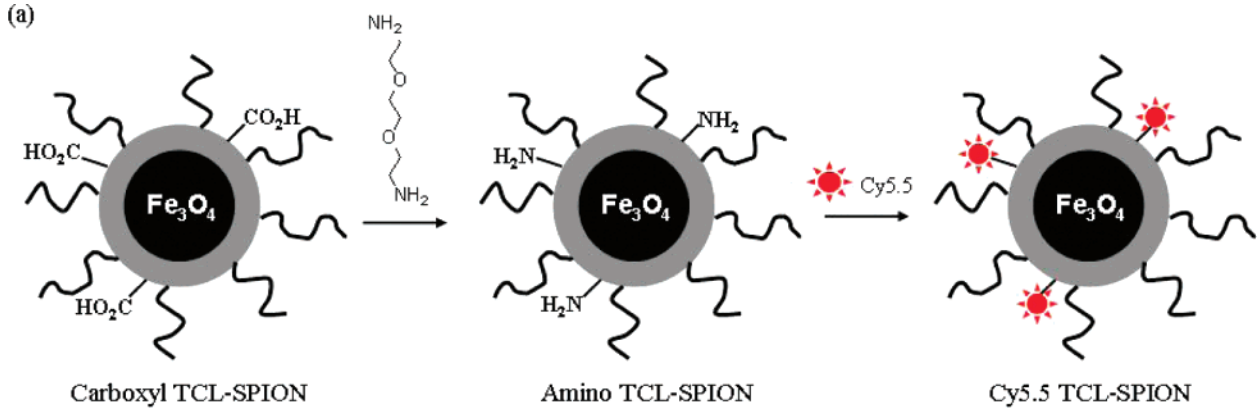

	Carboxyl TCL-SPION	Amino TCL-SPION	Cy5.5 TCL-SPION
Size (DLS)	25.6±2.7 nm	32.6±3.7 nm	31.9±4.6 nm
Zeta Potential	-30.50 mV	-1.34 mV	-25.13 mV

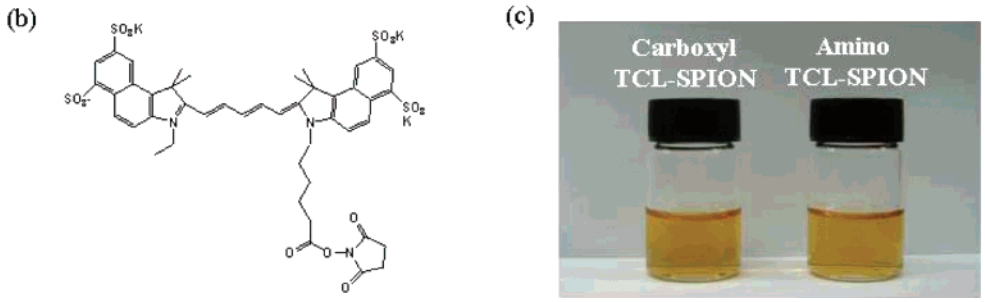

Figure 4. (a) Synthetic scheme for amino and Cy5.5 TCL-SPION with size and zeta potential changes. (b) Chemical structure of Cy5.5 mono NHS ester. (c) Photographs of carboxyl TCL-SPION and amino TCL-SPION dispersed in phosphate-buffered saline (pH 7.4).

high M_s of 77.5 emu/g of Fe (Figure S4, Supporting Information). It is noteworthy that the M_s value for TCL-SPION in this work is much larger than that for other polymer-coated SPION which possess approximately 30−50 emu/g of Fe.[16]

On the basis of previous studies of a similar polymer system, poly(TMSMA-*r*-PEGMA),[32] it is expected that $-Si(OH)_3$ groups of hydrolyzed poly(TMSMA-*r*-PEGMA-*r*-NAS) would be cross-linked upon heating, producing a highly stable polymer

coating that should be advantageous for its in vivo use. To determine whether the cross-linking reaction occurred, we analyzed the surface of the polymer-coated nanoparticles by XPS before and after a 2 h heat treatment at 80 °C. High-resolution Si(2p) XPS of the polymer-coated SPION before heat treatment showed four different types of Si(2p) peaks at 97.88, 99.36, 100.75, and 102.13 eV (Figure 3), which correspond to Si−metal (29.0%), Si(0) (17.8%), Si−OH (35.3%), and Si−O−C (17.9%), respectively. After heating, the peak corresponding to Si−OH significantly decreased from 35.3% to 28.9%, and a new peak characteristic of Si−O−Si bonds (12.5%) appeared at 101.46 eV, confirming cross-linking between Si−OH groups.

Because the carboxyl TCL-SPION has carboxylic acids groups on its surface, additional functions such as near-infrared dyes for optical imaging and cancer-specific ligands for targeting can be introduced.[35] According to previous literatures, with a dual MR/Optical imaging probe, it has been shown to get high sensitivity and spatial resolution.[35a] In addition, near IR imaging probes such as quantom dots can be used as a guidance during surgery by delineating the margins of tumors.[35b] In this report, as an example, we prepared TLC-SPION conjugated with the near-infrared dye Cy5.5 to examine the feasibility of the nanoparticle system as a dual (MR/optical) imaging probe for cancer in vivo.[35f,i] Although a few reports have described MR/optical-based dual imaging of cancer using multifunctional nanoparticles in vitro,[35c,g] to our knowledge, only few of the dual imaging of cancer in vivo has been reported using such nanoparticles.[35a,i]

Figure 4 depicts the synthetic scheme for the preparation of the Cy5.5-conjugated TCL-SPION. In the first step, the carboxyl TCL-SPION was converted to amino TCL-SPION after reaction with a hydrophilic bisamine reagent in aqueous solution. Next, NHS ester-activated Cy5.5 was reacted with the amino TCL-SPION to give covalently Cy5.5-conjugated TCL-SPION. We measured the particle sizes and zeta potentials of the nanoparticles at each step (Figure 4a). After amine modification, as expected, there was only a slight change in size (25.6 ± 2.7 vs 32.6 ± 3.7 nm), but there was a remarkable increase in zeta potential from −30 to −1 mV, indicating that the negatively charged carboxylic acid surface was converted to a positively charged, amine-modified surface. Cy5.5 modification, however, led to a decrease in zeta potential due to the attachment of the highly negatively charged dye to the particle surface. Measurement of the number of dye molecules per milligram of TCL-SPION revealed that approximately 0.02375 μg (0.021 nmol) of Cy5.5 dye was conjugated to each milligram of TCL-SPION (see Supporting Information, Figure S5). On the other hand, both carboxyl and amino TCL-SPION dispersed well in water and were stable for up to a month under ambient conditions without any sign of aggregation (Figure 4b). This high stability may be attributed to the existence of a firm, cross-linked polymeric coating layer on SPION.

We next performed in vivo cancer imaging using the Cy5.5-conjugated TCL-SPION. Cross-linked and anti-biofouling polymer coating layers of TCL-SPION have been shown to provide high stability in physiological medium and resistance to uptake by cells of the reticuloendothelial system such as macrophages.[15] Therefore, we expected that the Cy5.5-conjugated TCL-SPION upon systemic circulation could be increasingly accumulated at tumor tissues because blood capillary vessels supplying tumor

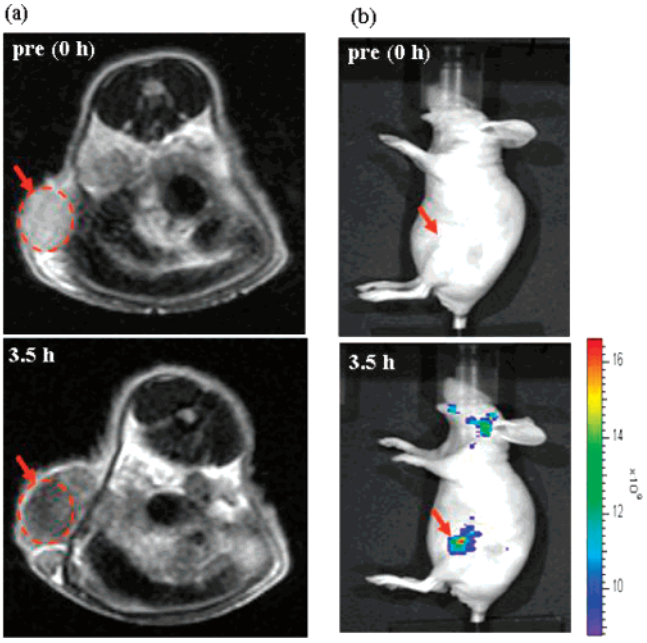

Figure 5. (a) T_2-weighted fast spin−echo images (TR/TE of 4200 ms/102 ms) taken at 0 and 3.5 h postinjection of 14.7 mg of Fe/kg of Cy5.5 TCL-SPION at the level of tumor (320 mm^3) on the flank above the upper left thigh of a nude mouse. The dashed circle with the red arrow indicates the allograft tumor region. (b) Optical fluorescence images of the same mouse taken at 0 and 3.5 h postinjection. Images were acquired with an exposure time of 1 s and with the Cy5.5 filter channel. The red arrows indicate the position of the allograft tumor. The colored scale indicates the relative fluorescence intensity.

tissue constitute leaky and porous vascular structures. This kind of passive tumor-targeting strategy is based on the enhanced permeability and retention effect and could be achieved if both sizes and surface properties of nanoparticles are rationally engineered.[38] Tumor-bearing mice were prepared by subcutaneous injection of LLC cells into the flank above their upper left thighs. MR and optical fluorescence images of the tumor-bearing mice were taken in a sequential manner at selected time points before and after intravenous injection of Cy5.5 TCL-SPION (14.7 mg Fe/kg) in phosphate-buffered saline.

Before injection of the Cy5.5 TCL-SPION, the tumor appears as a hyperintense area in T_2-weighted MR images (red arrow and dashed circle in Figure 5a). The relative signal intensity of the ROI in the T_2-weighted image was calculated. At 3.5 h postinjection of the Cy5.5 TCL-SPION, a noticeable darkening appeared in the tumor area in the T_2-weighted MR image. The mean decrease in signal was 68% compared to pre-injection, indicating a large accumulation of the SPION within the tumor. This decrease in signal is sufficient for a radiologist to detect the tumor with high confidence.

We also obtained in vivo fluorescence images of the same mouse at similar time points. At 3.5 h post-injection, the pseudocolor-adjusted optical images showed a relatively intense fluorescence signal exclusively in the tumor area (red arrow in Figure 5b). This finding agrees well with the MR imaging results. The fluorescence intensity measurement with times at the tumor areas revealed that t_{max}, the time when the accumulation of Cy 5.5 TCL-SPION at the area of interest is maximized,

(38) (a) Maeda, H.; Matsumura, Y. *Crit. Rev. Ther. Drug Carrier Syst.* **1989**, *6*, 193−210. (b) Matsumura, Y.; Maeda, H. *Cancer Res.* **1986**, *46*, 6387−6392.

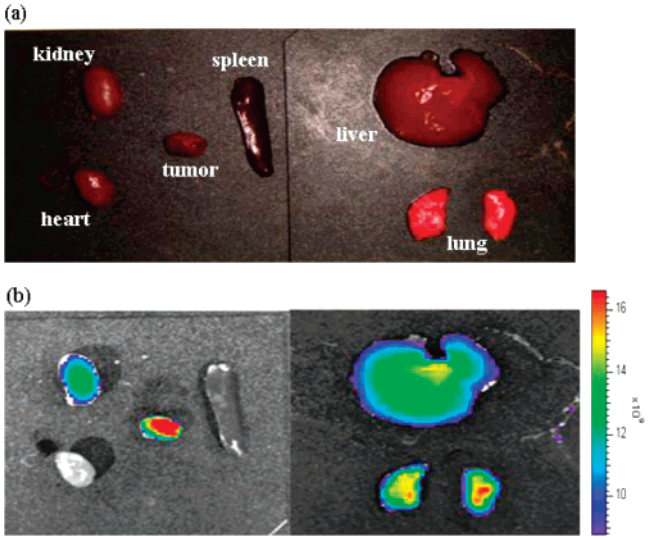

Figure 6. Photographic images (a) and corresponding optical fluorescence images (b) of several organs and the allograft tumor. The images were taken after sacrifice (at 3.5 h postinjection) of the same mouse that was used in the MR/optical imaging experiment (injected with 14.7 mg of Fe/kg of Cy5.5 TCL-SPION). Fluorescence images were acquired with an exposure time of 1 s and the use of the Cy5.5 filter channel. The colored scale indicates the relative fluorescence intensity.

was observed at 3 h after intravenous injection (Figure S8). Although the present SPION system does not have any specific targeting ligands on its surface, it appears to be the first successful use for MR/optical dual imaging of cancer in vivo by passive targeting based on the EPR effect.

Because the signal intensity of fluorescence images in vivo depends on the penetration of light, deep-positioned tissues or organs may not be easily visualized by fluorescent methods.[39] We therefore harvested several major organs from the same mouse after MR/optical imaging and collected fluorescence images ex vivo to verify the accumulation of TCL-SPION in the tumor (Figure 6). Consistent with the dual imaging results for whole mice, the highest fluorescence intensity was observed in the tumor. Although fluorescence was not detected in the heart and spleen, some fluorescence was observed in the kidney, liver, and lung. Because intravenously injected nanoparticles first arrive in the heart, followed by the lung, liver, and then other tissues, we suspected that some aggregated nanoparticles are filtered by the lung and liver, resulting in the accumulation of a fluorescent signal. When 5% glucose solution instead of PBS buffer was used for the Cy5.5 TCL-SPION injection, we could appreciably diminish the accumulation in liver but could not in lung (Figure S6). Despite this somewhat unfavorable biodistribution, the distinct difference in the relative accumulation between the tumor and other organs strongly suggests that these nanoparticles will be useful for dual imaging of cancer in vivo. On the other hand, when a free Cy5.5 dye was intravenously injected to tumor-bearing mice as a control experiment, we could see very little fluorescence signal in tumor but increased accumulation was observed in liver as well as lung as compared to that of Cy5.5 conjugated TCL-SPION (Figure S7). Overall results clearly indicate that the rationally engineered TCL-SPION is highly resistant to uptake by reticuloendothelial system organs such as liver and spleen and consequently circulates long enough to accumulate in tumor tissue.

(39) (a) Troy, T.; Jekic-McMullen, D.; Sambucetti, L.; Rice, B. *Mol. Imaging* **2004**, *3*, 9−23. (b) Weissleder, R. *Nat. Biotechnol.* **2001**, *19*, 316−317.

Conclusion

In conclusion, we fabricated a novel TCL-SPION containing functional groups, and demonstrated its potential use as a dual (MR/optical) imaging probe for cancer in vivo. Although Cy5.5-conjugated TCL-SPION does not possess any targeting ligands on its surface, it could efficiently detect tumors in vivo when analyzed by either MR or optical fluorescence imaging. Passive tumor targeting due to an enhanced permeability and retention effect could be achieved, presumably because of the antibiofouling and stable polymer coating layers on TCL-SPION. Because various functional molecules, such as targeting ligands and drugs, can be attached to the TCL-SPION, we are planning to develop multifunctional nanoparticles for cancer imaging and therapy as an extension of this work.

Acknowledgment. This study was supported by the Second Stage of Brain Korea 21 in Biology and a grant from the National Research and Development Program for Cancer Control, Ministry of Health and Welfare, Republic of Korea (0520080-1 and 0720210).

Supporting Information Available: The ^{1}H NMR spectrum of poly(TMSMA-*r*-PEGMA-*r*-NAS) and the FT-IR spectrum, TGA graph, magnetization of the carboxyl TCL-SPION, the fluorescence spectrum of Cy5.5 TCL-SPION, the in vivo MR/optical imaging data using Cy5.5 TCL-SPION dispersed in 5% glucose solution, the biodistribution of a free Cy5.5 dye, pharmacokinetics of Cy 5.5 TCL-SPION in tumor tissues and complete ref 5a, 10, 13, 14, 35b, 35c, and 35f. This material is available free of charge via the Internet at http://pubs.acs.org.

JA072210I